International Journal of Nanomedicine

Dovepress
open access to scientific and medical research

Open Access Full Text Article

ORIGINAL RESEARCH

Icariin-loaded porous scaffolds for bone regeneration through the regulation of the coupling process of osteogenesis and osteoclastic activity

This article was published in the following Dove Press journal:
International Journal of Nanomedicine

Yuanlong Xie[1,*]
Wenchao Sun[2,*]
Feifei Yan[1]
Huowen Liu[1]
Zhouming Deng[1]
Lin Cai[1]

[1]Department of Spine Surgery and Musculoskeletal Tumor, Zhongnan Hospital of Wuhan University, Wuhan City, Hubei Province, People's Republic of China; [2]Department of Pain Management, Wuhan Fourth Hospital, Wuhan City, Hubei Province, People's Republic of China

*These authors contributed equally to this work

Objective: Icariin (IC) promotes osteogenic differentiation, and it may be a potential small molecule drug for local application in bone regeneration. Icariin-loaded hydroxyapatite/alginate (IC/HAA) porous composite scaffolds were designed in this study for the potential application of the sustainable release of icariin and subsequent bone regeneration.

Methods: An icariin-loaded hydroxyapatite/alginate porous composite scaffold was prepared and characterized by SEM and HPLC for morphology and release behavior, respectively. The mechanical properties, degradation in PBS and cytotoxicity on BMSCs were also evaluated by MTT assay, compression strength and calculation of weight remaining ratio, respectively. Rabbit BMSCs were cocultured with IC/HAA scaffolds, and ALP activity and Alizarin Red staining were performed to evaluate osteogenic differentiation induction. The mRNA and protein expression level of an osteogenic gene was detected by RT-PCR and Western blotting, respectively. In vivo animal models of critical bone defects in the radius of rabbit were used. Four and 12 weeks after the implantation of IC/HAA scaffolds in the bone defect, radiographic images of the radius were obtained and scored by using the Lane and Sandhu X-ray scoring system. Tissue samples were also evaluated using H&E and Masson staining, and an osteogenic gene and Wnt signaling pathway genes were detected.

Results: A hydroxyapatite/alginate (HAA) porous composite scaffold-loaded icariin was fabricated using a freeze-drying method. Our data indicated that the icariin was loaded in alginate scaffold without compromising the macro/microstructure or mechanical properties of the scaffold. Notably, the IC/HAA promoted the proliferation of rBMSCs without exerting cytotoxicity on rBMSCs. In vivo, rabbit radius bone defect experiments demonstrated that the IC/HAA scaffold exhibited better capacity for bone regeneration than HAA, and IC/HAA upregulated the relative expression levels of an osteogenic gene and the Wnt signaling pathway genes. Most notably, the IC/HAA scaffold also inhibited osteoclast activity in vivo.

Conclusion: Our data suggests a promising application for the use of HAA scaffolds to load icariin and promote bone regeneration in situ through mediation of the coupling processes of osteogenesis induction and osteoclast activity inhibition.

Keywords: icariin, bone regeneration, osteogenesis, osteoclastic activity, drug delivery

Introduction

Bone defect treatment remains a significant clinical challenge for surgeons, particularly in regard to large segmental bone defects and the lack of vascular supply to the tissue.[1] Autografts and allografts remain the most common solutions in clinical applications, but these techniques are limited by immunological reactions, limited sources and risk of infection.[2] Biomaterial scaffolds for bone regeneration have

Correspondence: Lin Cai
Department of Spine Surgery and Musculoskeletal Tumor, Zhongnan Hospital of Wuhan University, 169 Donghu Road, Wuhan City, Hubei Province, People's Republic of China
Tel +86 0276 781 3116
Email orthopedics@whu.edu.cn

submit your manuscript | www.dovepress.com
DovePress
http://doi.org/10.2147/IJN.S203859

developed significantly over the last few decades.[3] A large amount of biomaterials including alginate, gelatin, collagen, silk protein, polymer, hydroxyapatite and β-tricalcium phosphate have been used for bone regeneration.[4,5] These scaffolds exhibit great advantages in osteoconductive and osteoinductive abilities, delivery of drugs or growth factors, and cell loading and revascularization.

Alginate is a biopolymer extracted from brown algae, and it has been actively examined in the preparation of scaffolds to facilitate bone regeneration with excellent biocompatibility.[6] Alginate scaffolds are frequently combined with inorganic materials, such as hydroxyapatite (HA), due to the lack of its mechanical strength in mimicking bone function. Alginate scaffolds with HA exhibited excellent applications in bone tissue engineering and the delivery of drugs and cells.[7] Hydroxyapatite enhanced the strength of the scaffold and bone formation through mimicking the native extracellular matrix of bone and promoted the adhesion of cells to the scaffold.[8,9]

Local drug delivery systems are applied for inducing and accelerating bone formation by releasing a variety of osteoinductive molecules such small molecules, DNA, RNA, proteins, etc.[10] Nevertheless, most of these small molecules are often easily degraded during the preparation process in vitro or fail in translational trials because of the unpredictable side effects.[11] BMP-2 protein delivery enhanced bone formation in bone defects, but some adverse effects were also reported, including ectopic ossification, soft tissue swelling, immune responses and an incidence of cancer.[12] Therefore, local delivery scaffolds should improve the availability and efficacy of osteogenesis, provide a continuous supply at the implant site, increase vascularization and reduce the adverse effects related to systemic administration.

Icariin (IC, C33H40O15, molecular weight: 676.67) is the main active natural flavonoid glucoside isolated from the herb Epimedium, and it is used because of its anti-osteoporosis and bone healing-enhancing effects.[13] Icariin exerts an effect on bone not only through the promotion of osteoblastogenesis, which leads to bone formation, but also through the suppression of osteoclastogenesis, which inhibits bone resorption.[14] Icariin promoted osteogenic differentiation by increasing ALP activity and upregulating the mRNA expression levels of Runx2, which is an osteoblast marker gene, BMP-2 and TGF-1.[15] Song et al.[16] reported that icariin increased MC3T3-E1 cell differentiation and mineralization via estrogen receptor-mediated ERK and JNK signal activation. As a potential small molecule drug, icariin exhibited a long-term effective controlled release using a natural scaffold of the small intestine submucosa.[17] And bone regeneration in a mouse calvarial defect model was accelerated by transplanting with icariin-calcium phosphate cement (CPC) tablets.[18]

The present study designed an icariin-loaded composite scaffold of hydroxyapatite/alginate to provide a sustainable release of icariin. We evaluated its characteristics, including pore size, morphology, mechanical properties, and the release behavior of icariin in vitro. In vitro osteogenic differentiation and in vivo bone regeneration were also investigated.

Materials and methods

Preparation of icariin-loaded hydroxyapatite/alginate porous composite scaffolds

Hydroxyapatite (HA, purity≥98.0%,<0.2 μm, CAS NO. 1306–06–5, medical grade, Aladdin, China) was added to deionized water (2 g:100 mL) under continuous stirring (magnetic stirrer, MS-H280-Pro, DLAB Scientific, China) at 200 rpm for 30 min. Alginate (CAS NO. 9005–38–3, endotoxin free, medical grade with a purity of 99%, Sigma-Aldrich, USA) was added (2 g:100 mL) under continuous stirring at 300 rpm for 6 h. This mixture was defined as the HAA solution. Icariin (CAS NO. 489–32–7, medical grade, ≥94.0%, Aladdin, China) was dissolved in anhydrous ethanol (1 mol: 1 L) to obtain the IC solution. The IC solution was slowly dissolved in the HAA solution at the ratio of 1 mL: 10^5 mL under continuous stirring for 6 h. $CaCl_2$ (2 wt%) was added to cross-link the mixed solution for 24 h to obtain the IC/HAA hydrogel. The IC/HAA hydrogel was frozen in a refrigerator at minus 20 °C for 2 h and was a microfuge (Thermo, America) at −80 °C overnight. To obtain dry IC/HAA scaffolds, the frozen IC/HAA hydrogel was immediately placed in a vacuum freeze drier (Labconco, USA) at minus 80 °C under vacuum. Three IC/HAA scaffolds with different concentrations of icariin (10^{-5}, 10^{-6}, and 10^{-7} mol/L) were made by adjusting the concentrations of icariin in the IC solution. The empty HAA scaffold was prepared as mentioned above without the addition of the IC solution. Co60 irradiation (20Gy) was applied to sterilize the composites.

Characterization of composites

Morphological observations and porosity measurement

The cross-sectional surface morphologies of the composites were observed by scanning elec tron microscopy (SEM,

TESCAN, Czech) after the samples were sputter-coated with gold under vacuum. The average pore size of the sectional composite surface was determined from the SEM photographs through an image analysis program that five selected SEM images were elvaluated using the linear intercept method. The porosity of samples was measured through ethanol displacement method based on Archimedes' Principle.[19] The following procedure was used for ethanol displacement: W_{b0} represents the weight of a bottle filled with ethanol. The sample was immersed in ethanol in the bottle until it was saturated from absorbing the ethanol. The samples were weighed and denoted as W_{s0}. The sample was re-immersed in ethanol in the bottle until it was saturated from absorbing the ethanol. The sample was removed, and the bottle with the remaining ethanol and the ethanol saturated sample were weighed and denoted as W_{b1} and W_{s1}, respectively. ρ is the ethanol density. The total volume of the sample including pores was calculated as $(W_{b0}- W_{b1})/\rho$, and the pore volume in the sample was $(W_{s1}- W_{s0})/\rho$. Each experiment was repeated three times. The reported data are the average of five samples. Therefore, the porosity of the sample was determined as follows:

$$\text{Porosity}(\%) = \frac{(Ws1 - Ws0)/\rho}{(Wb0 - Wb1)/\rho} \times 100\%$$

Degradation assay in PBS

In vitro degradation experiments were performed in PBS at 37 °C. HAA, 10^{-7}IC/HAA, 10^{-6}IC/HAA and 10^{-5}IC/HAA composites were dipped in 15-mL centrifuge tubes containing 10 mL PBS at 37 °C. The PBS was refreshed every week. The composites were removed, dried and weighed every week. Week 0 was defined as the baseline. The ratio of weight remaining was calculated as follows: Weight remaining ratio(%) $=(W_t/W_0)\times100\%$, where W_t and W_0 are the weights of the composites at setting time and baseline, respectively. Each experiment was repeated three times.

Mechanical properties of composites

The mechanical properties of the composites were generally measured by the compression strength in an Instron MicroTester (Instron, USA). The composites were compressed at a speed of 1 mm/min. The shape of samples for compression strength testing was 20 mm in length and 10 mm in diameter. The calculation of the compression strength followed the formula of compression strength= F/A, where F is the breakload and A the section area of the specimen.

In vitro release experiments

The release behavior of icariin from HAA scaffolds was measured by high-performance liquid chromatography (HPLC). Briefly, samples of IC/HAA were immersed in 5 mL PBS (pH 7.0) at 37 °C under gentle vibrating at 10 rpm. At the time points of 1, 2, 3, 10, 20, 30, and 40 days, the 5 mL PBS was collected and stored at 4 °C for HPLC examination. All samples were centrifuged at 3,000 rpm for 10 min, and 0.5 mL of the supernatants were isolated. Then, 0.5 mL of acetonitrile was added, and the mixture was recentrifuged at 6,000 rpm for 10 min. For analysis of icariin concentrations, supernatants were isolated for HPLC analysis. The column was a Waters SunFireTM C18 (250 mm × 4.6 mm, 5 μm), and the solvent was acetonitrile; the flow rate was 1 mL/min, and the column temperature was 40 °C. The detection wavelength was 270 nm, and the loading volume was 20 μl. The data for peak area integration were analyzed using Empower 2 software. Icariin release from the sample was calculated according to a standard curve, and the percentage of icariin released was calculated.

Cell culture and identification

The Animal Ethical Committee of Zhongnan Hospital of Wuhan University approved all animal experiments. BMSCs were obtained from 4-week-old rabbits as described previously. Briefly, rabbit femur bones were dissected from hind legs. Soft tissue and the periosteum were removed, and rabbit bone marrow samples were rinsed with PBS (pH 7.4) and centrifuged twice in PBS. Mononuclear cells (MNCs) were collected and plated in α-MEM medium supplemented with 10% FBS and 1% penicillin and streptomycin and cultured for 48 h at 37 °C in a humidified atmosphere of 5% CO_2. Adherent cells were collected as BMSCs and expanded in α-MEM medium for further study. The growth medium was replaced every other day, and all experiments were performed using BMSCs within passage five. The medium extract was prepared by soaking HAA (20 g) or IC/HAA (20 g) in 10 mL α-MEM for 4 weeks and filtered with a 100-μm sterile strainer mesh.

Cytotoxicity assay

The cytotoxicity of the composites on BMSCs was detected by the 3-(4,5-dimethylthiazol-2-yl)-2,5-diphenyltetrazolium bromide (MTT) assay. Briefly, BMSCs were seeded at 4000 cells per well in 100 μl cultured medium in

96-well plates and cultured for 24 h. The cells were exposed to α-MEM medium containing 10% (v/v) media extracts of HAA and IC/HAA. IC was used as the control. After 24 h, 48 h, 72 h, 96 h of incubation, 10 μL of MTT solution at a concentration of 5 mg/mL was added to each well, and the wells were incubated for an additional 4 h. Then, 150 mL of DMSO was added to each well to dissolve the formazan produced by intracellular mitochondrial dehydrogenases. The optical density of formazan salt in the 96-well plates was measured at 490 nm using a microplate reader (Thermo Scientific). Experiments were performed in sextuplicate.

Osteogenic differentiation detection

Alkaline phosphatase (ALP) staining and ALP activity assay

The osteogenic induction medium (OM) contained 10 nM of dexamethasone, 50 mg/mL of ascorbic acid 2-phosphate, and 10 mM of β-glycerophosphate in α-MEM-E medium containing 10% (v/v) media extracts of HAA and IC/HAA. Cells were cultured in OM for 21 days, and alkaline phosphatase (ALP) staining and ALP activity assays were performed to evaluate osteogenic differentiation. Briefly, cell samples were washed with PBS and fixed with 4% paraformaldehyde for 15 min at room temperature. The samples were washed with PBS twice and stained with 2-amino-2-methyl-1,3-propanediol aqueous solution containing fast blue salt and naphthol AS-MX phosphate for 15 min at room temperature. The samples were washed with PBS twice to remove the residual ALP staining solution and observed and photographed using an optical microscope. ALP activity was determined using a pNPP alkaline phosphatase assay kit (pNPP, Sigma-Aldrich, USA) according a previous protocol.[20] Briefly, cell samples were digested with 0.25% trypsin. The supernatant was collected and reacted with p-nitrophenylphosphate to release p-nitrophenol. The samples were collected and detected by microplate reader (Thermo Scientific) at 405 nm. ALP activity is expressed as IU/μg protein. Experiments were performed in triplicate.

Alizarin red staining

Cells were cultured in OM supplemented with 10% (v/v) media extracts of composites for 21 days, washed twice with PBS and fixed in 4% paraformaldehyde for 10 min. Samples were washed with deionized water and incubated with 1% Alizarin (pH 4.1) Red S solution for 10 min at room temperature. The plates were photographed under an optical microscope, and calcium deposits located in the orange and red positions were identified and calculated in each group. The deposited Alizarin Red S solution was collected and reacted with 10% cetylpyridinium chloride (Sigma-Aldrich) for 30 min. The mixture was placed in 96-well plates and detected by microplate reader at 620 nm for quantification of calcium deposition. Experiments were performed in triplicate.

Reverse transcription-polymerase chain reaction (RT-PCR) analysis

mRNA expression was analyzed by real-time PCR (RT-PCR). Total RNA were extracted from cells or tissue samples(radius bone) by TRIzol extraction method. After identification purity and concentration, RNA was reverse transcribed to cDNA using Super-Script III reverse transcriptase (Invitrogen, USA). Real-time PCR amplification was performed using a 7500 Real-Time PCR system (Applied Biosystems, USA). The mRNA expression level was normalized to the expression level of the housekeeping gene GAPDH. Relative gene expression levels were calculated using $2^{-\triangle\triangle Ct}$.[21] Each experiment was performed in triplicate. The following primers were used: Runx2 forward, 5′- GACTGTGGTTACCG TCATGGC −3′, reverse, 5′- ACTTGGTTTTTCATAACA GCGGA-3′; ALP forward 5′- TGGACCTCGTGGACAT CTG −3′, reverse, 5′- CAGGAGTTCAGTGCGGTTC −3′; OCN forward 5′- GAAGCCCAGCGGTGCA −3′, reverse, 5′- CACTACCTCGCTGCCCTCC −3′; Wnt3a forward 5′- CT GCGCCAACACAGAAATTATTGTA −3′, reverse, 5′- TTC ACTGGCATCTTCACTGATTCTT −3′; GSK3β forward 5′- GCGTGAGGAGGGATAAGG −3′, reverse, 5′- CAGTTGG TGGAAATAATAAAGG −3′; β-catenin forward 5′- GGAA ATCGTGCGTGACATTA −3′, reverse, 5′- GGAGCAATGA TCTTGATCTTC −3′; and GAPDH forward 5′- CCTCAAG ATTGTCAGCAAT −3′, reverse, 5′- ACCACAGTCCAT GCCATCAC −3′

Western blotting assay

Cells and tissue(radius bone) were lysed by RIPA buffer supplemented with a protease inhibitor cocktail for 30 min on ice. The lysate was collected and centrifuged at 12,000 g for 15 min. Protein in supernatant was collected and measured using the BCA assay for protein concentration detection. Each protein lysate was mixed with loading buffer at a ratio of 1:5 and denatured in boiling water. Each sample containing 20 mg protein lysate was loaded into the sample well of a polyacrylamide gel for SDS-PAGE electrophoresis. The proteins were

transferred to polyvinylidene difluoride membranes (PVDF, Millipore). The membranes were incubated with 5% skim milk for 1 h to block nonspecific interactions. The membranes were probed with specific primary antibodies against Runx2 (1:1,000), ALP (1:1,000), OCN (1:3,000), Wnt3a (1:2,000), GSK3β (1:2,000), -β-catenin (1:1,000), and GAPDH (1:5,000) overnight at 4 °C. Membranes were washed with a TBTS solution (15 min) three times and incubated with HRP-conjugated secondary antibodies (1:8000) for 4 h at room temperature. Bound antibodies were measured using an enhanced chemiluminescence detection system. Each experiment was performed in triplicate.

In vivo radius bone defects in rabbit

Animal model

All animal procedures were approved and performed following the Animal ethics committee of Wuhan University guidelines and complied with the ARRIVE guidelines. Twenty-four New Zealand rabbits (8 weeks) were randomly divided into four groups(n=6 in each group). All animals were anesthetized using 20 mg/kg pentobarbital sodium (1%) intravenously. Once the rabbits had reached a successful anesthesia, its right foreleg was shaved with an electric razor to remove the fur. The leg was washed using moist gauze and sterilized with 1% iodine solution. A 3.0 m full thickness skin incision was made longitudinally above the middle segment of the radius. A 2.0 cm bone defect in length was created in the middle segment of radius using an electric saw. Bone fragments and blood from the defect site were gently cleared with the aid of suction. Cobalt-60-sterilized IC/HAA and HAA were implanted using tweezers into the defect sites in IC/HAA and HAA group, respectively. The size of sample implanted in each group was 2×0.5×0.5 cm. Icariin was intravenously injected in the IC group, and nothing was implanted in the control group. Animals received intramuscular injections of penicillin G sodium (400,000 units per day) postoperatively for three consecutive days to prevent contamination of the operated site. Rabbits were housed in clean animal rooms and given access to food and water.

Radiographic imaging

To evaluate bone formation and union, plain radiographs were obtained using an X-ray unit (Philips Healthcare, Netherlands) and ultrahigh definition film; the parameters were 70 kV and 50 mA, and images were taken 4 and 12 weeks after surgery. New bone formation at postoperative timepoints of 4 and 12 weeks were scored in accordance with the modified Lane and Sandhu X-ray scoring system.[22] Three experts in the department of surgery, who were blind to the groups, performed the scoring.

Histological evaluations

The harvested implants were washed twice with normal saline, fixed in 4% paraformaldehyde at room temperature for 48 h and decalcified in EDTA for 4 weeks. The samples were dehydrated in a graded series of ethanol solutions, embedded in paraffin and sectioned to obtain cross-sections with a thickness of 5 μm. Cross-sections for morphological analyses were stained with Masson trichrome and hematoxylin & eosin (H&E, Japan). Cell nuclei were stained purple by hematoxylin, and the extracellular matrix was stained pink by eosin. Bone appeared as deep pink/red. Images of stained cross-sections were observed, acquired and digitized under a light microscope to evaluate the growth of normal bone tissues, osteogenic capacity, and lesions in surrounding tissues. The healing response in the H&E-stained samples was quantified by single blinded histomorphometric analyses. New bone was quantified through measuring the area of bone nucleation sites (BNS), and the bone defect margin was identified.[23] BNS was calculated in each section using ImageJ software with an automated method of pixel saturation quantification. Images were captured with an optical microscope, and the level of bone tissue regeneration was calculated according to Lane-Sandhu histological scoring criteria.[24] Each experiment was performed in triplicate.

Statistical analysis

All experiments were repeated a minimum of three times. Experimental results are presented as the means ± the standard deviation (SD). Data were analyzed by a two-tailed Student's *t*-test as appropriate for the data set. A p-value <0.05 was considered statistically significant.

Results

Characterization of IC/HAA composites

SEM was used to observe the surface morphology and structure of the HAA and three IC/HAA scaffolds containing different concentrations icariin. The SEM micrographs (Figure 1A) showed that the dimension of interconnected pores was approximately 50–350 μm in the four types of composites. Analysis of the pore sizes showed that the pore sizes were 247.3±38.9, 252.9±36.8, 255.7±41.3, and 241.5 ±35.1 μm. The porosities (%) of HAA, 10^{-7} IC/HAA, 10^{-6} IC/HAA, and 10^{-5} IC/HAA scaffolds were 87.36±0.38,

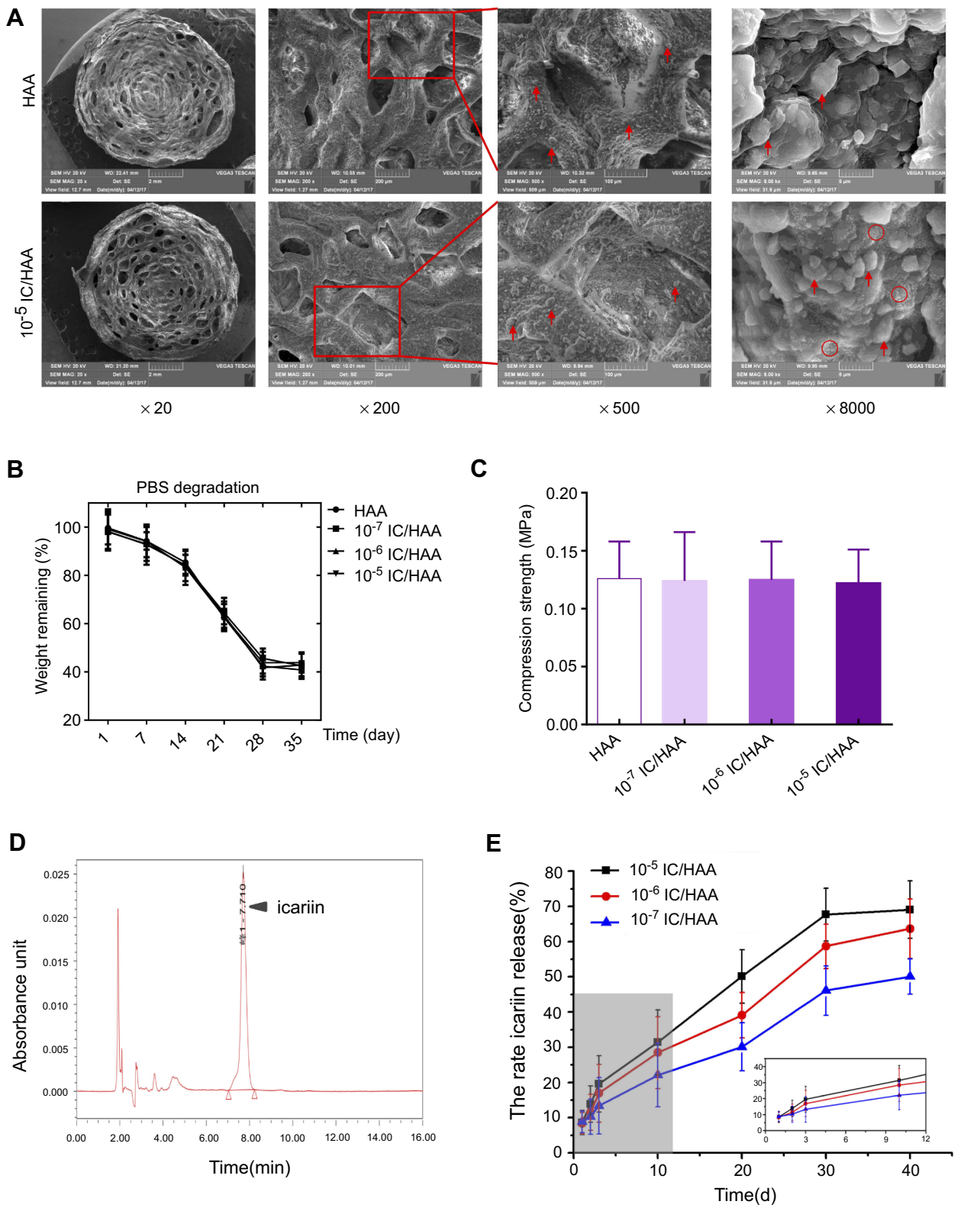

Figure 1 Characterization of IC/HAA composite. (**A**) SEM images of the IC/HAA scaffolds. Red arrow indicates the nanohydroxyapatite. Red circle indicates the icariin. (**B**) Degradation assay in PBS. (**C**) Compression strength of the scaffolds. (**D** and **E**) HPLC detection of icariin release from IC/HAA composite scaffolds. (**D**) Representative HPLC image of the 10^{-5} IC/HAA scaffold. (**E**) Statistical linear graph of the release rate(%) of icariin in each group.

88.99±0.44, 86.75±0.56, and 87.34±0.49%, respectively, as listed in Table 1. No significant differences in porosity or pore size were detected between the four groups. No significant differences in the degradation rates in PBS were

Table 1 Porosity and pore size of HAA and IC/HAA

Sample	Porosity (%)	Pore size (μm)
HAA	87.36±0.38	247.3±38.9
10^{-7} IC/HAA	88.99±0.44	252.9±36.8
10^{-6} IC/HAA	86.75±0.56	255.7±41.3
10^{-5} IC/HAA	87.34±0.49	241.5±35.1

found among the four scaffolds (Figure 1B). After 28 days of degradation assay in PBS, the ratio of weight remaining in each group was near 40%. A mechanical compression test was performed to detect the compression strength of the scaffolds (Figure 1C). The compression strength of HAA, 10^{-7} IC/HAA, 10^{-6} IC/HAA, and 10^{-5} IC/HAA scaffolds were 0.126±0.032, 0.124±0.042, 0.125±0.033, and 0.122 ±0.029 Mpa, respectively. No significant differences in compression strength were observed among the four groups.

The loading amounts of icariin in the HAA, 10^{-7} IC/HAA, 10^{-6} IC/HAA, and 10^{-5} IC/HAA scaffolds were 0, 10^{-5}, 10^{-6}, and 10^{-7} mol/L, respectively. The release of icariin was observed using HPLC over a 40-day period (Figure 1D and E). The absorption peak of HAA appeared at 2 min, and the absorption peak of icariin appeared at 7.8 min (Figure 1D). The cumulative release percentage of icariin from the IC/HAA scaffolds was calculated based on the icariin loading amount, and the icariin release percentage increased with the increasing of icariin loading amount. When the release test was carried out to 30 days, the icariin release percentage of three scaffolds reached a plateau. After 40 days, the cumulative icariin release percentages from 10^{-7} IC/HAA, 10^{-6} IC/HAA, and 10^{-5} IC/HAA scaffolds were 50.09±5.03%, 63.68±8.46%, and 69.07±8.16%, respectively (Figure 1E). The 10^{-5} IC/HAA scaffold exhibited the highest release percentage of the three scaffolds; therefore, the 10^{-5} IC/HAA may be considered the optimal loading concentration for the IC/HAA scaffold.

In vitro bioactivity

Cytotoxicity assay

The 10^{-5} IC/HAA scaffolds were cultured with BMSCs for 24 h, 48 h, 72 h, and 96 h to determine cytotoxicity. The MTT assay showed that the optical density values at 570 nm at 24 h, 48 h, 72 h, and 96 h in the IC group and 10^{-5} IC/HAA scaffold (IC/HAA) group were significantly higher than the control group (Figure 2A). The optical density values of the HAA scaffold without icariin were also higher than the control group at 48 h, 72 h, and 96 h. The optical density values in the IC/HAA group at 24 h, 48 h, 72 h, and 96 h were significantly higher than the IC group. These results suggest that IC/HAA, IC, and HAA promoted the proliferation of BMSCs instead of inducing cytotoxicity.

Osteogenic differentiation detection

ALP activity detection showed that the staining intensity in BMSCs cultured with IC/HAA was obviously stronger than the IC, HAA and control groups (Figure 2B). Similarly, Alizarin Red staining and ALP staining showed that the staining intensity of IC/HAA was obviously stronger than the other three groups (Figure 2C). Slightly more intense staining of ALP or Alizarin Red was observed in the IC group compared to the HAA group. The results of ALP activity detection (Figure 2B) and quantification of mineralization (Figure 2D) corresponded well with the ALP staining and Alizarin Red staining, respectively. These results suggested that HAA scaffolds loaded with icariin produced significant stimulation of the osteogenic differentiation of rBMSCs.

The expression levels of osteogenic marker genes (Runx2, ALP, and OCN) and the Wnt signaling pathway genes (Wnt3a, GSK3β, β-catenin) in rBMSCs was analyzed by RT-PCR and Western blotting after a 21-day culture with the scaffolds (Figure 3A–C). The relative protein and mRNA expression levels of Runx2, ALP, OCN, Wnt3a, GSK3β, and β-catenin were upregulated by IC/HAA compared to the HAA, IC and control groups. The relative protein and mRNA expression levels of Runx2, ALP, OCN, Wnt3a, GSK3β, and β-catenin in the IC group was higher than the HAA group. HAA also upregulated the osteogenic marker genes compared to the control group, but no significant differences were observed in the relative protein and mRNA expression levels of Wnt3a, GSK3β, or β-catenin between the HAA and control groups. These results indicated that the scaffolds containing icariin exhibited better stimulatory effects on the relative expression levels of osteogenic and Wnt signaling pathway genes. HAA alone did not stimulate the relative expression levels of the Wnt signaling pathway.

In vivo study results

Gross appearance and radiographic results

To determine the effect of icariin sustained release and osteogenic effects on bone regeneration, the HAA and IC/HAA scaffold constructs were implanted into the bone defect sites of a rabbit radius for 4 and 12 weeks. An equivalent concentration of icariin was intravenously injected in the IC group, and nothing was implanted in the control group. The

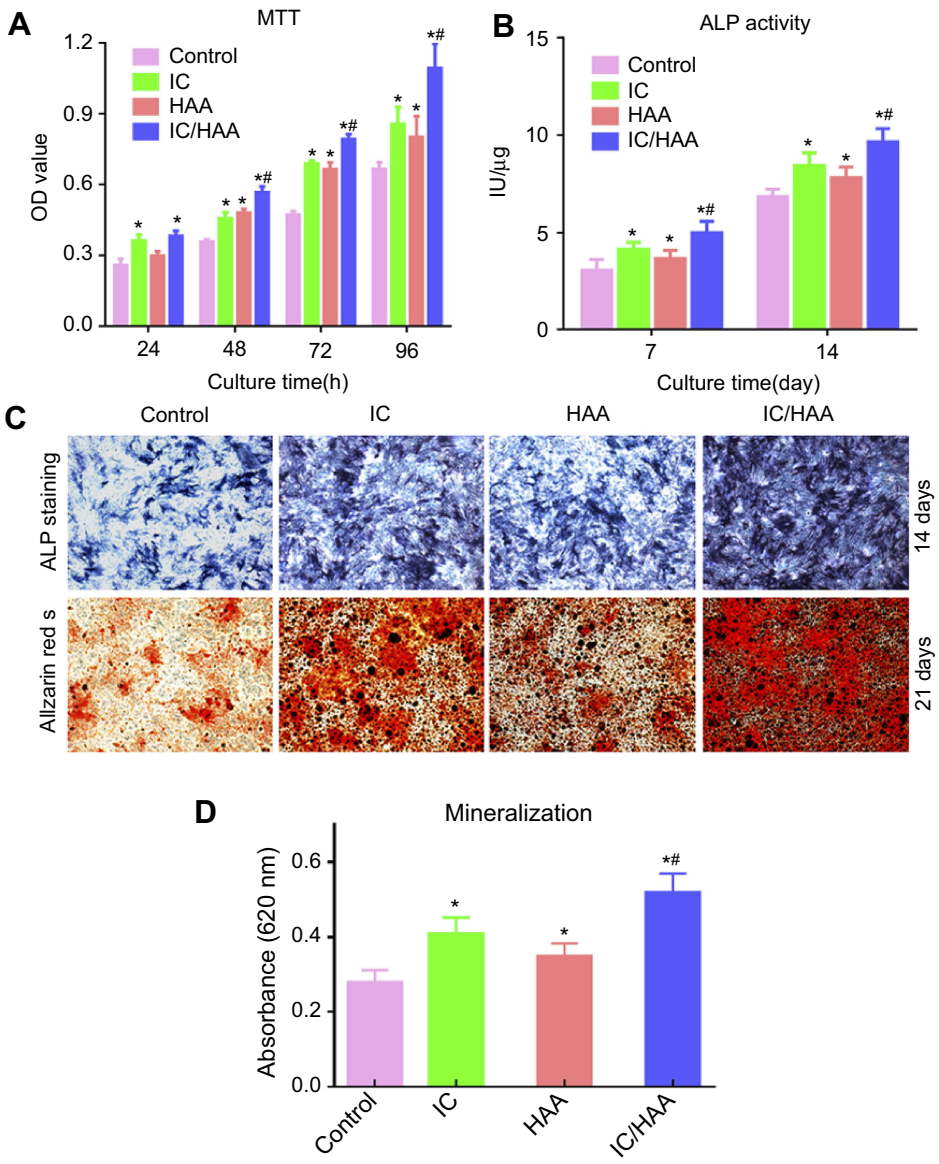

Figure 2 Cytotoxicity assay and osteogenic differentiation detection. (**A**) The optical density (OD) values of the MTT assays in the four groups. (**B, C** and **D**) Osteogenic differentiation detection in each group. (**B**) ALP activity in each group. (**C**) ALP staining and Alizarin Red S in each group. (**D**) Mineralization detected by measurement of the absorbance at 620 nm.

Notes: *P<0.05, compared with control group, #P<0.05, compared with HAA group.

gross appearance of the bone defect sites after 4 and 12 weeks are shown in Figure 4A. Photographs of X-rays in each group are shown in Figure 4B. The radiographic Lane-Sandhu scoring of bone defect sites in the IC/HAA, HAA, and IC groups increased significantly compared to the control group after 4 and 12 weeks (Figure 4C). The radiographic Lane-Sandhu scoring of the IC/HAA group was significantly higher than the HAA and IC groups.

Histological results

H&E and Masson staining showed that new bone formation was observed in the three groups 4 weeks after implantation, but this formation was not evident in the control group (Figure 5A). The signs of new bone formation in the IC/HAA implant group were more evident than the IC injection group and HAA group. Plenty of fibrous tissue and fatty tissue filled in the bone defect sites in IC injection group and control group. The in-growth of new blood vessels was more abundant in the IC/HAA group than the other three groups. The histological scoring was significantly highest in the IC/HAA group of the four groups. Histological scoring was higher in the HAA and IC groups than the control group at 4 and 12 weeks (Figure 5C). Residual nondegraded HAA scaffolds were observed in

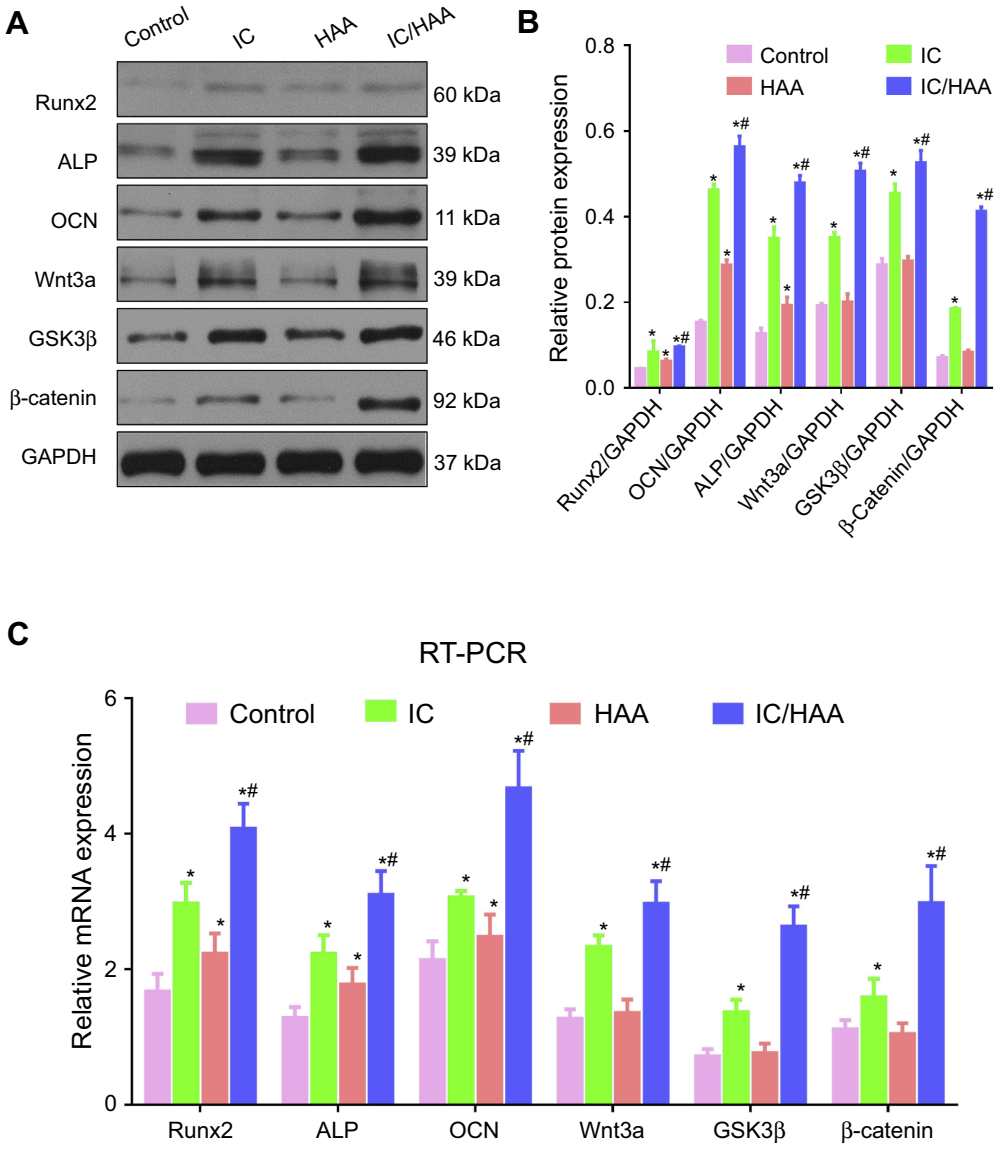

Figure 3 The expression levels of osteogenic marker genes (Runx2, ALP, and OCN) and Wnt signaling pathway genes (Wnt3a, GSK3β, and β-catenin) in rBMSCs was analyzed by RT-PCR and Western blotting. (**A** and **B**) Western blotting assays for protein expression detection. (**A**) Representative Western blotting band in each group. (**B**) Histogram of the relative protein expression level in each group. (**C**) Relative mRNA expression level in each group.
Notes: *P<0.05, compared with control group, #P<0.05, compared with HAA group.

the IC/HAA and HAA groups. New bone and vessel formation became more obvious 12 week after implantation compared to the 4-week implants, especially in the IC/HAA group (Figure 5B). Figure 5D shows the TRAP staining of tissue samples in each group. The numbers of osteoclasts in the IC group and IC/HAA group were significantly lower than the control group. These results indicated that icariin suppressed osteoblastic activity.

Osteogenic marker and Wnt signaling pathway gene expression levels

The mRNA and protein expression levels of the osteogenic marker genes (Runx2, ALP, and OCN) and the Wnt signaling pathway (Wnt3a, GSK3β, and β-catenin) in the bone regeneration area at 12 weeks were analyzed by RT-PCR and Western blotting, respectively (Figure 6A–C). The relative protein and mRNA expression levels of Runx2, ALP, OCN, Wnt3a, GSK3β, and β-catenin were upregulated in the IC/HAA group compared to the HAA, IC and control groups. The relative protein and mRNA expression levels of Runx2, ALP, and OCN in the IC and HAA groups were higher than the control group, and the relative expression levels in the IC group was lower than the HAA group. Notably, the relative protein and mRNA expression levels of Wnt3a, GSK3β, and β-catenin in the IC group were significantly higher than the

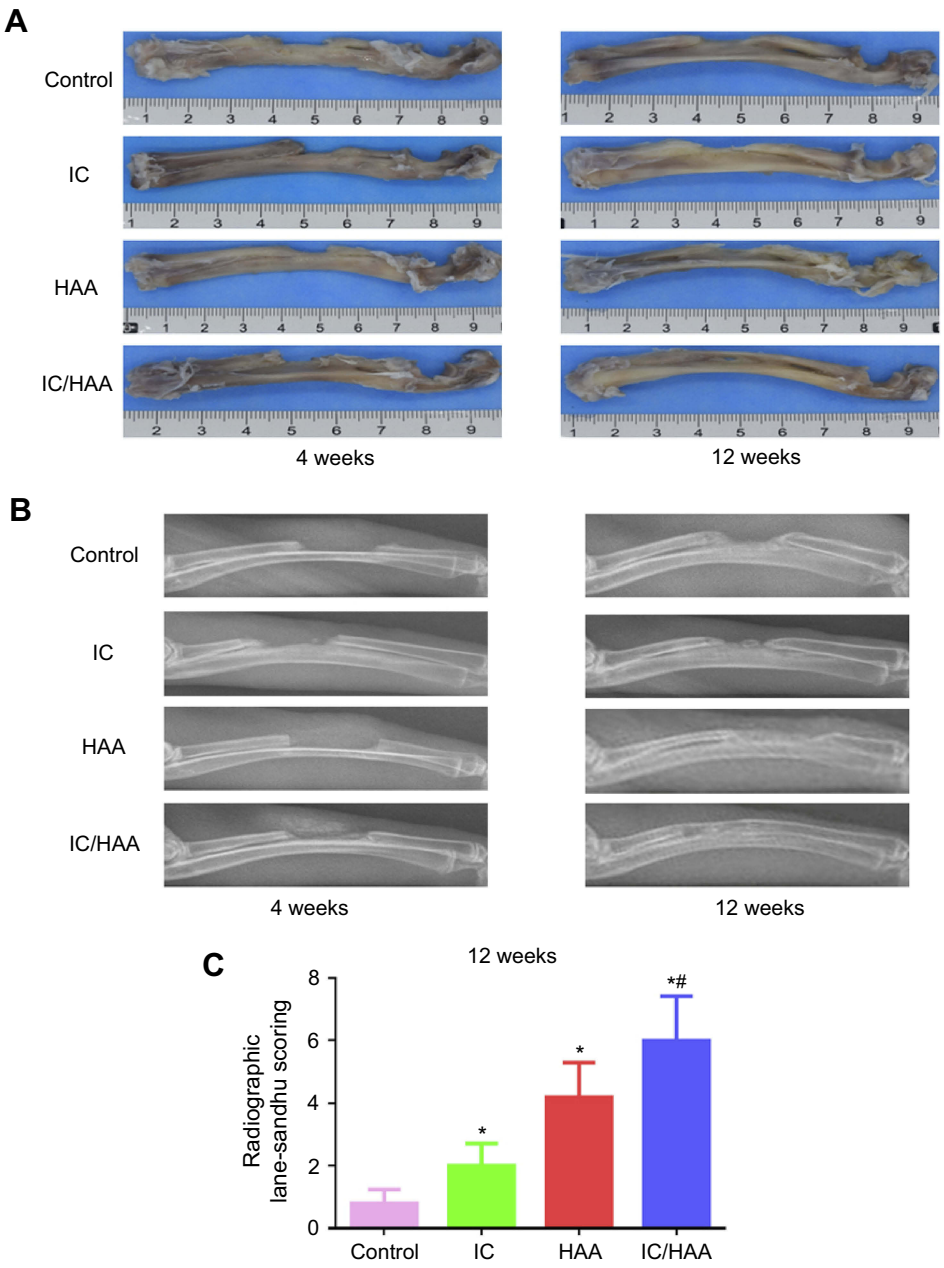

Figure 4 Animal experiments of scaffold implantation in rabbit radius bone defect. (**A**) Gross appearance of the bone defect sites after 4 and 12 weeks. (**B**) Photographs of X-rays in each group after 4 and 12 weeks. (**C**) Radiographic Lane-Sandhu scoring of bone defect sites in the IC/HAA, HAA, and IC groups, (n=6).
Notes: *$P<0.05$, compared with control group, #$P<0.05$, compared with HAA group.

control group, but no significant differences were observed between the HAA and control groups. These results indicated that local icariin injection, HAA and IC/HAA promoted the expression of osteogenic marker genes, and IC/HAA possessed the strongest promotion observed in of the groups. Icariin but not HAA upregulated the Wnt signaling pathway, which facilitates bone formation.

Discussion

As a novel type of drug delivery scaffold for icariin, IC/HAA exhibited the high porosity (87.34±0.49) and interconnected pore structure (dimensions approximately 50–350 μm). Lin et al.[25] reported that the pore size of scaffolds at the midsection was approximately 178 μm at a −80 °C freezing temperature, which is similar to our result. It has been reported

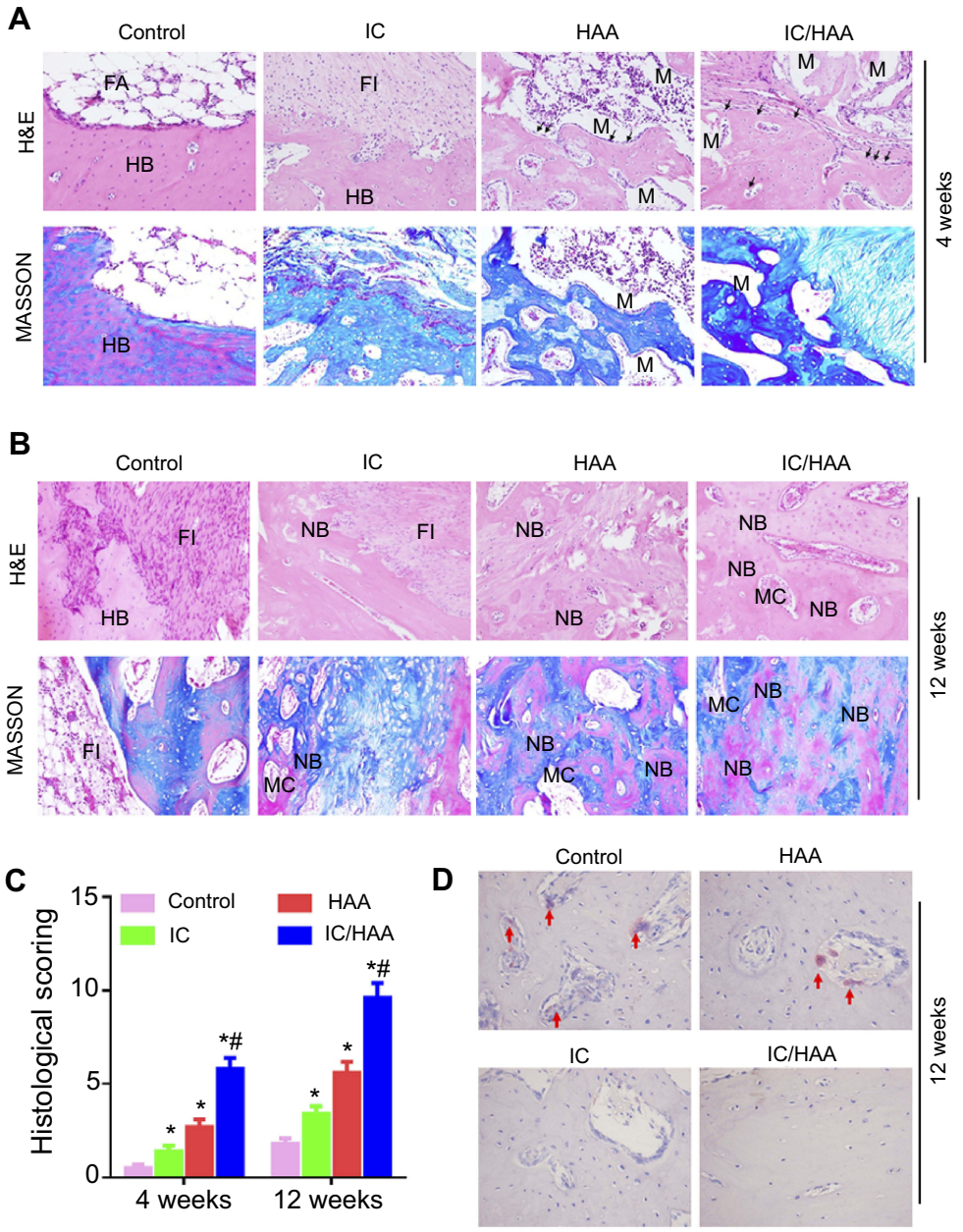

Figure 5 Histological evaluations of bone defect sites at 4 and 12 weeks. (**A**) H&E and Masson staining of bone defect sites in each group at 4 weeks. (**B**) H&E and Masson staining of bone defect sites in each group at 12 weeks. (**C**) Histological scoring of bone regeneration in each group at 4 and 12 weeks. (**D**) TRAP staining of tissue samples from each group.

Notes: Red arrows indicate osteoclast. *P<0.05, compared with control group, #P<0.05, compared with HAA group.

Abbreviations: HB, host bone; NB, new bone; MC, marrow cavity; FI, fibrous tissue.

that the requirement for pore size is similar to 100 μm due to cell size, migration and transport. Therefore, the porous structure of IC/HAA would provide a specific three-dimensional microenvironment for cell adhesion, migration and growth. The encapsulation of icariin in an HAA scaffold did not affect the compressive strength of HAA. The compressive strength of IC/HAA was greatly stronger than the porous alginate scaffolds for cells culture. The ideal scaffold for bone regeneration must exhibit a biodegradation rate that corresponds to bone remodeling speed.[26] The mechanical properties of IC/HAA fully satisfy the requirements of regeneration for bone defects in nonweight bearing areas, where adequate mechanical support is not necessary. IC/HAA exhibited a controlled release of icariin for at least 30 days in vitro. The duration of sustained icariin release beneficially matches the time period of bone regeneration. The first

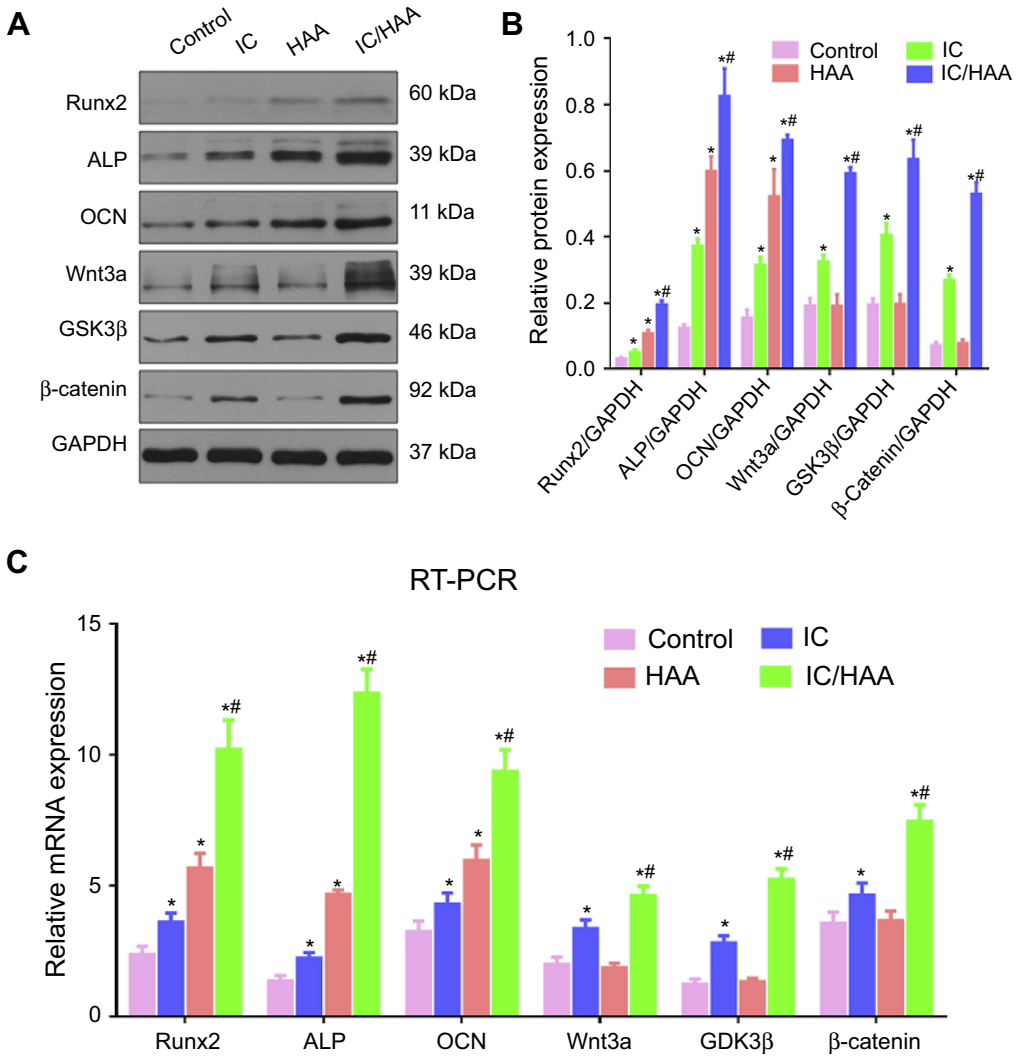

Figure 6 The mRNA and protein expression levels of the osteogenic marker genes (Runx2, ALP, and OCN) and Wnt signaling pathway genes (Wnt3a, GSK3β, and β-catenin) in the bone regeneration area at 12 weeks. (**A** and **B**) Western blotting assays of protein expression. (**A**) Representative Western blotting bands in each group. (**B**) Histogram of relative protein expression in each group. (**C**) Relative mRNA expression in each group at 12 weeks.
Notes: *$P<0.05$, compared with control group, #$P<0.05$, compared with HAA group.

4 weeks are the most important for the critical physiological process of bone repair, including stem cell recruitment, callus growth, osteogenic differentiation and calcification. Local active factors are more beneficial for the critical physiological processes than the bone remodeling process after the initial 4 weeks. The MTT assay also confirmed that the IC/HAA produced no cytotoxicity in the rabbit BMSCs. Therefore, the IC/HAA may be a feasible bone repair material.

The delivery of growth factors is a promising approach for the repair of bone defects, but much improvement is needed in the control of delivery mechanisms (sequence, dose and timing) and kinetics.[10,23] It is important to preserve the bioactivity of the bone regeneration stimulator during the procedure of scaffold fabrication.[27] The in vivo and in vitro experiments in the present study demonstrated the biological activity of icariin in the scaffold. IC/HAA, HAA and icariin accelerated the osteogenic differentiation of rabbit BMSCs, but the effect of IC/HAA on osteogenic differentiation was the strongest in vitro. The IC/HAA scaffold was implanted into the bone defect in the radius of rabbits to evaluate the osteogenic potential of the IC/HAA scaffold in vivo. X-ray and histology analyses demonstrated that the loading of icariin into the HAA scaffold facilitated bone defect regeneration.

The dose of local administration was equal to the scaffold material, and the efficacy of local icariin administration was of short duration because of the scavenging

and metabolism of body fluids.[28] The in vivo results of the present study showed that IC/HAA was more effective than IC alone, which confirmed that IC/HAA sustainably released icariin. Icariin administered locally may be more efficient for local bone regeneration than a systemic administration because the gastrointestinal and cardiovascular barriers may reduce the therapeutic efficacy of icariin given systemically. The most common problem of growth factor delivery is the appropriate release kinetics provided by the suboptimal delivery systems. Numerous delivery materials are far from ready for clinical use, but the commercially and clinically available options, rather than novel and experimental delivery systems, are potential candidates as a delivery material. Hydroxyapatite and alginic acid are widely used as scaffold materials,[29,30] and the present study confirmed that icariin exhibited good biological activity in these scaffolds in vivo and in vitro.

Hydroxyapatite also induces osteogenesis, but the knowledge of the mechanisms and pathways for induction of osteogenesis and the role of inducing osteogenic differentiation of BMSCs is limited.[31] Hydroxyapatite is more of a biological skeleton material.[32] The results of gene expression from the animal experimental specimens showed that hydroxyapatite promoted the expression of osteogenic marker genes, but it did not promote the genes of the Wnt signaling pathway, and icariin explicitly promoted both the osteogenic and Wnt signaling pathways. Therefore, icariin is indeed an excellent active component for bone regeneration. Animal experimental histology also showed that the biomaterials loaded with icariin did not induce excessive inflammatory cells to interfere with osteogenesis and promoted vascularizations.

Bioactive agents are critical for the effects of tissue engineering techniques. Icariin stimulates the osteogenic differentiation of BMSCs into osteoblasts through multiple signaling pathways, including BMP (bone morphogenetic protein),[33] NO (nitric oxide),[34] MAPK (mitogen-activated protein kinase),[35] and the canonical Wnt/β-catenin pathways.[36] Icariin treatment of preosteoblastic MC3T3-E1 cells and mouse primary osteoblasts in vitro promotes the expression of osteoblast marker genes, Runx2 (runt-related transcription factor 2) and Id-1 (inhibitor of DNA-binding 1).[37] Notably, icariin and IC/HAA scaffolds but not the HAA scaffold stimulated the canonical Wnt/β-catenin pathways in the present study. Icariin also facilitates the maturation of primary osteoblasts and bone remodeling activity of osteoblasts. Scaffold slow-release of icariin induced the expression of terminal differentiation markers ALP (alkaline phosphatase), OCN and Runx2 in our study. Further, it has been demonstrated that new bone formation was detected in β-TCP ceramic scaffolds loaded with icariin but not in β-TCP ceramic scaffolds alone after intramuscular implantation in the backs of rats for three months.[38] Ectopic bone formation strongly demonstrated the potential for osteoinduction of icariin.

The phytomolecule icariin promotes bone formation through enhancing of osteoblastic differentiation, mineralization, and vascularization and the inhibition of osteoclastic activity.[39] Incorporation of icariin into an HAA scaffold greatly advanced osteoblastic differentiation and mineralization of BMSCs cultured with the scaffold. Alginate was actually designed to mediate a sustained release of bioactive substances, and it is used as a drug delivery system.[40] The HAA scaffold expands with water immersion, and the icariin encapsulated in the HAA is released. This release is quick and may be seen initially after ten days. The release of icariin from the HAA scaffold lasted at least 4 weeks. The structural integrity of IC/HAA scaffolds gradually disappeared with the dissolution of the HAA scaffold; thus, the icariin incorporated inside the scaffolds also dissolved into the PBS solution. Furthermore, bioactive substances were loaded into alginate to protect the substances from rapid enzymatic degradation and metabolization in vivo. The complete exposure of icariin to fluid environments in vivo resulted in a substantial loss of bioactivity. Owing to the encapsulation of icariin in the HAA scaffold, the local release of icariin was sustained for longer than 40 days in vitro; thus, the IC/HAA composite may exhibit long-term efficacy in enhancing the repair of bone defects.

Conclusion

The present study described the preparation of a novel hydroxyapatite- alginate scaffold containing icariin (IC/HAA) for the repair of critical-sized bone defects through osteoinduction, osteoconduction, and activation of genes for osteogenic differentiation. The scaffold provided efficient, localized and sustained delivery of therapeutics with no evidence of an excessive inflammatory response, which supports its effective function and safety. Most notably, the scaffold showed a coupling process of osteogenesis induction and osteoclast activity inhibition because of the biological function of icariin. Therefore, this cell-free icariin-carrying scaffold may be used as a clinical treatment for bone defects in non-load-bearing areas.

Acknowledgments

This study was funded by the Science and Technology Innovation Team Training Plan of the Wuhan Science and Technology Foundation (Grant No. 2015070504020231), the Breeding Key Project of Research and Development Plan of the Zhongnan Hospital of Wuhan University (Grant No. znpy2016060) and Health Care of Yellow Crane Talent Plan of Wuhan City (Grant No. 17). The authors declare no competing financial interests.

Disclosure

The authors report no conflicts of interest in this work.

References

1. Reynolds JJ, Khundkar R, Boriani S, et al. Soft tissue and bone defect management in total sacrectomy for primary sacral tumors: a systematic review with expert recommendations. *Spine*. 2016;41(Suppl 20):S199–S204.
2. Wang W, Yeung KWK. Bone grafts and biomaterials substitutes for bone defect repair: A review. *Bioact Mater*. 2017;2(4):224–247. doi:10.1016/j.bioactmat.2017.05.007
3. Ghassemi T, Shahroodi A, Ebrahimzadeh MH, Mousavian A, Movaffagh J, Moradi A. Current concepts in scaffolding for bone tissue engineering. *Arch Bone Jt Surg*. 2018;6(2):90–99.
4. Elgali I, Omar O, Dahlin C, Thomsen P. Guided bone regeneration: materials and biological mechanisms revisited. *Eur J Oral Sci*. 2017;125(5):315–337. doi:10.1111/eos.12364
5. Noori A, Ashrafi SJ, Vaez-Ghaemi R, Hatamian-Zaremi A, Webster TJ. A review of fibrin and fibrin composites for bone tissue engineering. *Int J Nanomedicine*. 2017;12:4937–4961. doi:10.2147/IJN.S124671
6. Venkatesan J, Bhatnagar I, Manivasagan P, Kang KH, Kim SK. Alginate composites for bone tissue engineering: a review. *Int J Biol Macromol*. 2015;72:269–281. doi:10.1016/j.ijbiomac.2014.07.008
7. Ren X, Sun Z, Ma X, et al. Alginate-mediated mineralization for ultra-fine hydroxyapatite hybrid nanoparticles. *Langmuir*. 2018. doi:10.1021/acs.langmuir.8b00151
8. Ma B, Han J, Zhang S, et al. Hydroxyapatite nanobelt/polylactic acid janus membrane with osteoinduction/barrier dual functions for precise bone defect repair. *Acta Biomater*. 2018;71:108–117. doi:10.1016/j.actbio.2018.02.033
9. Didier P, Piotrowski B, Fischer M, Laheurte P. Mechanical stability of custom-made implants: numerical study of anatomical device and low elastic young's modulus alloy. *Mate Sci Eng C Mater Biol Appl*. 2017;74:399–409. doi:10.1016/j.msec.2016.12.031
10. Martin V, Bettencourt A. Bone regeneration: biomaterials as local delivery systems with improved osteoinductive properties. *Mate Sci Eng C Mater Biol Appl*. 2018;82:363–371. doi:10.1016/j.msec.2017.04.038
11. Wang Y, Newman MR, Benoit DSW. Development of controlled drug delivery systems for bone fracture-targeted therapeutic delivery: A review. *Eur J Pharm Biopharm*. 2018;127:223–236. doi:10.1016/j.ejpb.2018.02.023
12. El Bialy I, Jiskoot W, Reza Nejadnik M. Formulation, delivery and stability of bone morphogenetic proteins for effective bone regeneration. *Pharm Res*. 2017;34(6):1152–1170. doi:10.1007/s11095-017-2147-x
13. Wang Z, Wang D, Yang D, Zhen W, Zhang J, Peng S. The effect of icariin on bone metabolism and its potential clinical application. *Osteoporos Int*. 2018;29(3):535–544. doi:10.1007/s00198-017-4255-1
14. Indran IR, Liang RL, Min TE, Yong EL. Preclinical studies and clinical evaluation of compounds from the genus Epimedium for osteoporosis and bone health. *Pharmacol Ther*. 2016;162:188–205. doi:10.1016/j.pharmthera.2016.01.015
15. Wang Q, Cao L, Liu Y, et al. Evaluation of synergistic osteogenesis between icariin and BMP2 through a micro/meso hierarchical porous delivery system. *Int J Nanomedicine*. 2017;12:7721–7735. doi:10.2147/IJN.S141052
16. Song L, Zhao J, Zhang X, Li H, Zhou Y. Icariin induces osteoblast proliferation, differentiation and mineralization through estrogen receptor-mediated ERK and JNK signal activation. *Eur J Pharmacol*. 2013;714(1–3):15–22. doi:10.1016/j.ejphar.2013.05.039
17. Li M, Gu Q, Chen M, Zhang C, Chen S, Zhao J. Controlled delivery of icariin on small intestine submucosa for bone tissue engineering. *Mate Sci Eng C*. 2017;71:260–267. doi:10.1016/j.msec.2016.10.016
18. Zhao J, Ohba S, Komiyama Y, Shinkai M, Chung UI, Nagamune T. Icariin: a potential osteoinductive compound for bone tissue engineering. *Tissue Eng Part A*. 2010;16(1):233–243. doi:10.1089/ten.TEA.2009.0165
19. Oh SH, Park IK, Kim JM, Lee JH. In vitro and in vivo characteristics of PCL scaffolds with pore size gradient fabricated by a centrifugation method. *Biomaterials*. 2007;28(9):1664–1671. doi:10.1016/j.biomaterials.2006.11.024
20. Balmayor ER, Geiger JP, Aneja MK, et al. Chemically modified RNA induces osteogenesis of stem cells and human tissue explants as well as accelerates bone healing in rats. *Biomaterials*. 2016;87:131–146. doi:10.1016/j.biomaterials.2016.02.018
21. Xie Y, Sun W, Deng Z, Zhu X, Hu C, Cai L. MiR-302b suppresses osteosarcoma cell migration and invasion by targeting Runx2. *Sci Rep*. 2017;7(1):13388. doi:10.1038/s41598-017-13353-9
22. Zhou J, Lin H, Fang T, et al. The repair of large segmental bone defects in the rabbit with vascularized tissue engineered bone. *Biomaterials*. 2010;31(6):1171–1179. doi:10.1016/j.biomaterials.2009.10.043
23. Raftery RM, Mencia Castano I, Chen G, et al. Translating the role of osteogenic-angiogenic coupling in bone formation: highly efficient chitosan-pDNA activated scaffolds can accelerate bone regeneration in critical-sized bone defects. *Biomaterials*. 2017;149:116–127. doi:10.1016/j.biomaterials.2017.09.036
24. Lane JM, Sandhu HS. Current approaches to experimental bone grafting. *Orthop Clin North Am*. 1987;18(2):213–225.
25. Lin HR, Yeh YJ. Porous alginate/hydroxyapatite composite scaffolds for bone tissue engineering: preparation, characterization, and in vitro studies. *J Biomed Mater Res B Appl Biomater*. 2004;71(1):52–65. doi:10.1002/jbm.b.30065
26. Polo-Corrales L, Latorre-Esteves M, Ramirez-Vick JE. Scaffold design for bone regeneration. *J Nanosci Nanotechnol*. 2014;14(1):15–56.
27. van Griensven M. Preclinical testing of drug delivery systems to bone. *Adv Drug Deliv Rev*. 2015;94:151–164. doi:10.1016/j.addr.2015.07.006
28. Li M, Zhang C, Zhong Y, Zhao J. A novel approach to utilize icariin as icariin-derived ECM on small intestinal submucosa scaffold for bone repair. *Ann Biomed Eng*. 2017;45(11):2673–2682. doi:10.1007/s10439-017-1900-y
29. de Almeida AD, Leite FG, Chaud MV, et al. Safety and efficacy of hydroxyapatite scaffold in the prevention of jaw osteonecrosis in vivo. *J Biomed Mater Res B Appl Biomater*. 2018;106(5):1799–1808.
30. Kolmas J, Pajor K, Pajchel L, et al. Fabrication and physicochemical characterization of porous composite microgranules with selenium oxyanions and risedronate sodium for potential applications in bone tumors. *Int J Nanomedicine*. 2017;12:5633–5642. doi:10.2147/IJN.S140935

31. Li D, Liu H, Zhao J, et al. Porous lithium-doped hydroxyapatite scaffold seeded with hypoxia- preconditioned bone-marrow mesenchymal stem cells for bone-tissue regeneration. *Bioact Mater*. 2018;13(5):055002.
32. Choi S, Friedrichs J, Song YH, Werner C, Estroff LA, Fischbach C. Intrafibrillar, bone-mimetic collagen mineralization regulates breast cancer cell adhesion and migration. *Biomaterials*. 2019;198:95–106.
33. Wu JZ, Liu PC, Liu R, Cai M. Icariin restores bone structure and strength in a rat model of chronic high-dose alcohol-induced osteopenia. *Cell Physiol Biochem*. 2018;46(4):1727–1736. doi:10.1159/000489248
34. Zhai YK, Guo XY, Ge BF, et al. Icariin stimulates the osteogenic differentiation of rat bone marrow stromal cells via activating the PI3K-AKT-eNOS-NO-cGMP-PKG. *Bone*. 2014;66:189–198. doi:10.1016/j.bone.2014.06.016
35. Qin S, Zhou W, Liu S, Chen P, Wu H. Icariin stimulates the proliferation of rat bone mesenchymal stem cells via ERK and p38 MAPK signaling. *Int J Clin Exp Med*. 2015;8(5):7125–7133.
36. Liu Y, Huang L, Hao B, et al. Use of an osteoblast overload damage model to probe the effect of icariin on the proliferation, differentiation and mineralization of MC3T3-E1 cells through the Wnt/beta-catenin signalling pathway. *Cell Physiol Biochem*. 2017;41(4):1605–1615. doi:10.1159/000470896
37. Zhao J, Ohba S, Shinkai M, Chung UI, Nagamune T. Icariin induces osteogenic differentiation in vitro in a BMP- and Runx2-dependent manner. *Biochem Biophys Res Commun*. 2008;369(2):444–448. doi:10.1016/j.bbrc.2008.02.054
38. Zhang X, Guo Y, Li DX, et al. The effect of loading icariin on biocompatibility and bioactivity of porous beta-TCP ceramic. *J Mater Sci*. 2011;22(2):371–379. doi:10.1007/s10856-010-4198-y
39. Lai Y, Cao H, Wang X, et al. Porous composite scaffold incorporating osteogenic phytomolecule icariin for promoting skeletal regeneration in challenging osteonecrotic bone in rabbits. *Biomaterials*. 2018;153:1–13. doi:10.1016/j.biomaterials.2017.10.025
40. Ciriza J, Saenz Del Burgo L, Gurruchaga H, et al. Graphene oxide enhances alginate encapsulated cells viability and functionality while not affecting the foreign body response. *Drug Deliv*. 2018;25(1):1147–1160. doi:10.1080/10717544.2018.1474966